JCTC Journal of Chemical Theory and Computation

Article

pubs.acs.org/JCTC

Free Energies by Thermodynamic Integration Relative to an Exact Solution, Used to Find the Handedness-Switching Salt Concentration for DNA

Joshua T. Berryman* and Tanja Schilling

University of Luxembourg, Luxembourg

Supporting Information

ABSTRACT: Sets of free energy differences are useful for finding the equilibria of chemical reactions, while absolute free energies have little physical meaning. However finding the relative free energy between two macrostates by subtraction of their absolute free energies is a valuable strategy in certain important cases. We present calculations of absolute free energies of biomolecules, using a combination of the well-known Einstein molecule method (for treating the solute) with a conceptually related method of recent genesis for computing free energies of liquids (to treat the solvent and counterions). The approach is based on thermodynamic integration from a detailed atomistic model to one which is simplified but analytically solvable, thereby giving the absolute free energy as that of the tractable model plus a correction term found numerically. An example calculation giving the free energy with respect to salt concentration for the B- and Z-isomers of all-atom duplex DNA in explicit solvent and counterions is presented. The coexistence salt concentration is found with unprecedented accuracy.

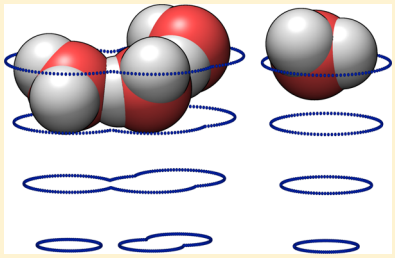

INTRODUCTION

Overview. Recent improvements of atomistic force fields for nucleic acids[1] and advances in a particular family of thermodynamic integration techniques[2−5] together encourage a return to what we believe should be considered, due to its combination of simplicity and intractability, as a canonical model system to benchmark computational methods for biomolecules and polyelectrolytes: the handedness-switching B to Z isomerization of DNA.

Here, we present a new addition to the progression of free energy methods beginning from the "Einstein Crystal" of Frenkel and Ladd,[6] followed by the "Einstein Molecule,"[7] the "Confinement Method,"[3] and a recently introduced analytical reference-liquid model.[5,8] We demonstrate this new method using the example of the transition between B and Z DNA. In the absence of an existing umbrella term for this philosophy of free energy calculation, it is referred to here as Thermodynamic Integration relative to an Exact Solution (TIES) because it relies on performing a Thermodynamic Integration (TI) calculation with a realistic (but intractable) model at one end point of the integration path and an exactly solvable (ES) model at the other. The principal technical advance within the field of TIES to be presented here is in the adaptation of a recently developed reference liquid model[5,8] such that it can be used for triangular water in a molecular dynamics simulation and successful combination of this adapted liquid model with the existing Einstein Molecule (EM) model for the solute.

For the "realistic," but intractable, end of the integration path, the AMBER simulation code[9] and selected AMBER force field parameters were used. The details of this quantitative all-atom treatment (with Coulomb, bonded, and van der Waals interactions) are given in the Methods.

The results of the example calculation are found to be of groundbreaking accuracy for the example considered, although they were computationally expensive, and the scope for future gains in efficiency is acknowledged.

B−Z DNA Isomerization. The B−Z isomerization of duplex DNA is a gross structural transition, from a right-handed double helix (the canonical B-form) to a left-handed double helix (the Z-form, which occurs *in vitro* at high salt concentration[10,11] or *in vivo* with the assistance of DNA-binding proteins[12] and/or with negative supercoiling[13]). The occurrence of Z-DNA in mammalian cells has been implicated as a causative factor for certain cancers.[14] In low salt, the (more compact) Z-DNA is disfavored relative to B-DNA for reasons of electrostatics and solvation; it becomes free energetically favorable in total when a high salt concentration screens the repulsion between the charged backbone phosphate groups, also making partial solvent-exposure of the base pairs more favorable (Figure 1). The unwinding which is required to change the handedness of the double helix presents a formidable energetic barrier which must be overcome for the transition to take place,[15,16] even when the ends of the duplex are free.

The salt concentration for coexistence of these two forms is known from circular dichroism measurements to be roughly 2.8 M NaCl for $[d(CG)]_6$; this varies with sequence, temperature, chain length, and methylation.[10,11,17] The availability of these experimental data, particularly for short dodecamer sequences, has attracted several simulation studies. Definitive thermodynamic characterization with respect to salt concentration has

Received: July 13, 2012
Published: November 19, 2012

dx.doi.org/10.1021/ct3005968 | J. Chem. Theory Comput. 2013, 9, 679−686

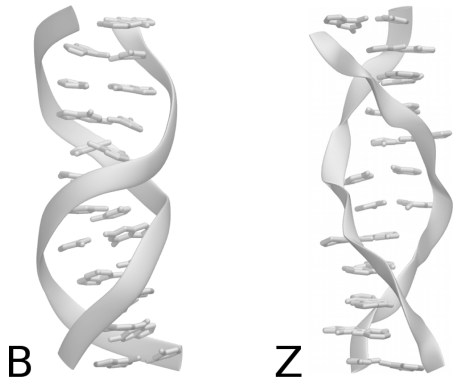

Figure 1. B and Z isomers of $[d(CG)_6]_2$ DNA, after 12 ns equilibration in 1 M NaCl. The backbone phosphate groups are closer together in the more compact Z isomer, and the base stacks have greater solvent exposure.

remained just over the horizon for some years; however recent improvements have been made: 3DRISM has been qualitatively successful in finding the coexistence point[18] (estimated at 0.8 M), and targeted molecular dynamics simulations have had at least some success in describing the transition path,[15,16] although this last matter is still difficult to compare directly against experimental results.

Previous Calculations of the Energetics. The history of computational studies of the B−Z transition from a free energy point of view is, in a microcosm, the history of developing computational methods for molecular electrostatics and solvation. Early treatments used continuum electrostatic models and rigid-body treatments of the DNA, either based on static atomic structures[19,20] or on geometric constructs such as grooved cylinders[21] or double-helical chains of charged beads.[22] A review article in 1987[23] pointed out that results from continuum-electrostatics seemed to depend dramatically on the assumptions made for the various geometric and physical parameters. The same review article also ruled out an all-atom simulation approach for the near future on grounds of computational expense (a view still advanced some 23 years later by researchers from another group[18]).

A paper in 1997[24] responded to the perceived limitations of a continuum treatment of the ions, by making a hybrid approach with discrete counterions in continuum solvent. The same paper pointed out that treatments which give a coexistence concentration without calculating the nonelectrostatic free energy difference are either right for the wrong reasons (if they ignore this contribution) or cheating somewhat, by setting the nonelectrostatic free energy change to whatever value gives the correct coexistence point (e.g., ref 21). In the "right for the wrong reasons" category falls one of the most accurate results, based on a classical density-functional theory (DFT) approach, which gave qualitative agreement of 3.6 M NaCl to the infinite-chain coexistence value of 2.25 M as early as 1989;[25] however the model used was without any detailed representation of the DNA. When the same author returned to the problem 21 years later with a similar but more detailed model taking into account the atomic structure of the water molecules and the DNA, the final value for the coexistence was in fact less accurate than the older one,[18] at 0.8 M (compared to the dodecamer coexistence value of 2.8 M), although of course more insight was available from the use of the richer model.

The calculation we present gives the most accurate value for the position of this conformational equilibrium from an all-atom treatment, and also the most accurate without fitting parameters to date (yielding a coexistence concentration of 2.5 M NaCl compared to the 2.86 M observed experimentally by Pohl and Jovin in 1972[10]). With the understanding that calculations from other methods can of course provide insight in different ways, the previous values reported in the literature were, in chronological order, 2.25 M[22] (exactly right for the infinite chain, but with Na^+ hard-sphere radius set as a free parameter to 4.95 Å vs the crystal ionic radius of 0.12 Å[26]), 3.6 M (vs 2.25 M for the infinite chain),[25] no transition,[24] 3.7 M (vs 2.4 M given by them as the infinite-chain value),[21] and 0.8 M[18] (vs 2.86 for the dodecamer).

Given the difficulty of finding the correct coexistence value, some papers have drawn attention to the gradient of the free energy with respect to concentration, comparing their results with a fit to the empirical data of

$$\beta\Delta G_{B-Z} = A \ln \frac{[Na^+]}{C} \tag{1}$$

where $\beta = 1/k_BT$, ΔG_{B-Z} is the free energy difference per base pair, and C is the coexistence concentration.[27] This fit was derived based on data at the long-chain limit ($A = 0.6$, $C = 2.25$). There has not been a great deal more success from theory in matching the observed gradient $\partial\beta\Delta G/\partial \ln[Na^+]$ of the free energy near coexistence than the coexistence point itself, and the fit of a simple logarithm to the free energy has been brought into question by more recent experimental work pointing to the existence of intermediates.[28,29]

The gradients near coexistence of some reported theory treatments were $A = 0.3$,[20] $A = 0.15$,[24] and $A = 0.3$.[21] One theory treatment gave an elbow in the plot, with a value below coexistence of approximately $A = 0.3$ and above coexistence of $A = 0.6$.[22]

Thermodynamic Integration Relative to Exact Solution. This established and powerful family of thermodynamic integration (TI) techniques has recently been extended to permit application to liquids.[3,5,8] In brief, the method consists of defining for a given system a reference Hamiltonian $\mathcal{H}_1(\vec{r},\vec{p})$ which has an analytically tractable expression for its free energy (described in the Supporting Information) and also a realistic but intractable $\mathcal{H}_0(\vec{r},\vec{p})$ (here, the AMBER Hamiltonian). A third, "mixed" Hamiltonian is then defined as a sum of the two:

$$\mathcal{H}(\vec{r}, \vec{p}, \lambda) = f_0(\lambda)\,\mathcal{H}_0(\vec{r}, \vec{p}) + f_1(\lambda)\,\mathcal{H}_1(\vec{r}, \vec{p}) \tag{2}$$

Here, λ is introduced as a control variable of the system such that for $\lambda = 0$, $f_0(\lambda) = 1$ and $\mathcal{H}(\vec{r},\vec{p},0) = \mathcal{H}_0(\vec{r},\vec{p})$, while for $\lambda = 1$, $\mathcal{H}(\vec{r},\vec{p},1) = \mathcal{H}_1(\vec{r},\vec{p})$. The Helmholtz free energy A_0 of the system under the realistic (but intractable) Hamiltonian $\mathcal{H}_0$ can then be expressed in terms of an integral with respect to λ:

$$A_0 = A_1 - \int_0^1 d\lambda < \frac{\partial}{\partial\lambda}\mathcal{H}(\vec{r}, \vec{p}, \lambda)>_{N,V,T,\lambda} \tag{3}$$

where A_1 and $\mathcal{H}_1$ refer to the free energy and Hamiltonian of the reference system, $f_0(\cdot)$ and $f_1(\cdot)$ are mixing functions used to control the speed with which $\mathcal{H}_1$ is introduced in place of $\mathcal{H}_0$ over the interval $\lambda = [0,1]$, and $\langle\rangle_{N,V,T,\lambda}$ refers to the ensemble average for a given value of λ. Each "generalized force" $\langle\partial/(\partial\lambda)\mathcal{H}(\vec{r},\vec{p},\lambda)\rangle_{N,V,T,\lambda}$ is found by collecting time averages of the partial derivatives of $\mathcal{H}$ while the system evolves under this mixed Hamiltonian at fixed λ. (Here, obviously, the sampling times need to be long enough to allow for identification of the ensemble average with the time

dx.doi.org/10.1021/ct3005968 | J. Chem. Theory Comput. 2013, 9, 679−686

average.) While the time-averaged generalized force may be slow to converge, this procedure has the advantage that calculations at each value of λ can be carried out in parallel, without any need for intercommunication.

Einstein Molecule and Cage-Swapping Liquid Model. The first presentation of TIES was in the context of an $\mathcal{H}_1$ appropriate for solids or for macromolecules in a vacuum, due to Frenkel and Ladd[6] with modifications by Vega and Noya,[7] and is known as the "Einstein Molecule method" (EM) or as "the confinement method." The basic idea of the EM reference model is that the particles do not interact with each other, so that the reference partition function factorizes and the reference free energy can easily be computed exactly. In the simplest such model, the particles are simply coupled to predetermined reference positions by harmonic springs.

The EM model was used here for the DNA chains. The reference model used for the water and counterions in this calculation, however, is still quite new and has been slightly modified from its most recent appearance in the literature[8] for use in conjunction with MD rather than Monte Carlo sampling.

The EM model of harmonic wells cannot be used unmodified as a reference for the liquid state. In the liquid, each particle is ultimately free to move throughout the volume; so the range of the harmonic well in the EM model would have to be infinite as well. Thus to sample the average in eq 3, one would need to sample for infinite lengths of time. Instead, we use a potential which is attractive at a short range from the reference position but flat at long range (Figure 2). The

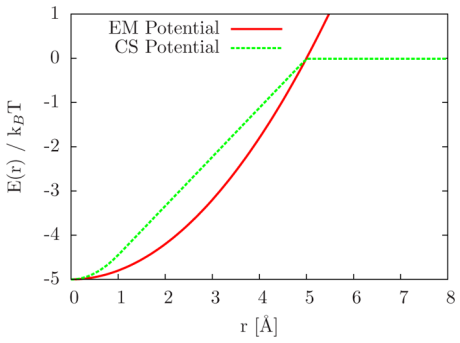

Figure 2. A simple harmonic well was used for the EM potential, while a constant-force well with a cutoff at long range and a harmonic region at very short range was used for the CS potential of the fluid part of the system.

contribution of the flat part to the partition function of the mixed model is trivial, so there is no need to extensively sample the reference model outside the short range of attraction.

The use of a potential cutoff solves the problem of dealing with an infinitely ranged well of attraction, but it introduces another problem: for a large system volume, a diffusing particle hardly ever revisits its reference site, once it has left the attractive well. We solve this problem by means of a Monte Carlo move in which we swap particle identities such that the diffusing particle has frequent opportunities (via a Metropolis acceptance rule) to rejoin or part from its reference site. This model is here called "CS," with reference to the "Cage-Swapping" dynamical behavior which it provides. The "cage-swapping" move reflects the factorial term in the general partition function of liquids, related to the indistinguishability of particles. For a detailed explanation, see Schilling and Schmid.[5]

The alternative in the literature to the CS MC move is to solve the linear assignment problem of particle identities so as to minimize the particle-well interaction energy at each MD time step, as by Tyka et al.[3] (see also ref 30). This has both advantages and drawbacks over the approach of using an MC move, and a thorough comparison might be valuable in a later publication. The principal advantage of linear assignment appears to be that the size of the configuration × identity space is reduced because the system always has the identity assignment which gives the mininum energy for the given configuration. The principal advantage of MC cage-swapping would appear to be enhanced sampling, as nearby particles can exchange wells even if it is not energetically favorable to do so, with the well exchange creating an attractive force which pulls the particles to their new minima.

Modifications made for the MD/MC CS model used here relative to previous pure-MC treatments were to use MD time steps instead of those MC moves which moved particles spatially without changing their identities, and to add a harmonic region near the well-bottoms, such that the wells were harmonic out to 1 Å, then constant force out to 5 Å, and then flat. The small harmonic region was necessary for the stability of the MD.

A natural objection to the use of a swap move in conjunction with MD simulation is to ask if it is required that the MC sampling should converge before each MD time step takes place; mercifully it has been shown in other work that any combination of MD and MC steps which would individually provide Boltzmann sampling of the degrees of freedom to which they are applied will in total provide Boltzmann sampling of the combined degrees of freedom.[31]

Detailed Motivation of the Integration. In a TI calculation, the free energy landscape of the system gradually morphs from one shape to another, in a way that is not yet easy to characterize. From an intuitive basis, we can state qualitatively that for effective TI, four sometimes-conflicting criteria are important: (a) To minimize the error from the numerical integration, the integration path should be as smooth as possible, meaning that the higher-order derivatives of each generalized force $\partial/(\partial\lambda)f(\lambda)\mathcal{H}$ should be as small as possible. (b) The shapes of landscapes to be mixed should be similar to each other, otherwise the generalized force due to $\mathcal{H}_0$, for instance, could sporadically take extremely large values when $f_0(\lambda)$ is small and $\mathcal{H}_1$ is primarily controlling the dynamics. (c) To minimize the convergence time per integration point, exploration of the mixed landscapes should be as fast as possible. (d) Because the variance of the generalized force scales with the gradient of the mixing function $f(\lambda)$, to efficiently distribute sampling between integration points, the mixing functions should be as close to linear as is consistent with the other criteria.

To meet criterion a, it is first required to avoid discontinuities in the generalized forces by making sure that the integration does not cross any first order phase transitions. The basis of TIES is a successful treatment of this issue by defining tractable models which match a given phase in terms of the symmetries expressed by their partition functions. Definition of the model partition functions is discussed in the Supporting Information.

Criterion b is more difficult. The reference model that we use decouples all particles from each other (in this way, the partition function is easily solved analytically). Thus, at $\lambda = 1$ particles can freely move through each other, while for $\lambda = 0$ this is not possible. Therefore the landscape under $\mathcal{H}_1$ is

dx.doi.org/10.1021/ct3005968 | J. Chem. Theory Comput. 2013, 9, 679−686

topologically different from that under $\mathcal{H}_0$. This brings the question of appropriately changing between landscapes sharply into focus. In order to treat cases where a cavity in the free energy landscape (e.g., a region of infinite potential energy, such as due to the Lennard-Jones short-range repulsion) must be introduced, starting from a flat potential, it is valuable to gradually increase the maximum energy associated with that region to some high but finite value. The region is only then blocked completely, by introducing the infinite potential inside the region which is already effectively forbidden by the large finite potential. This strategy, which was attempted here by use of the "Guide Hamiltonian" discussed below, should ensure that regions of phase space which are populated for a given λ are also populated at neighboring values of λ, while still allowing topological change of the landscape to occur. In the absence of such a technique, the generalized force can diverge, with an infinitesimal change in λ giving an infinite change in $\mathcal{H}\partial/(\partial\lambda)f(\lambda)$.

A further, partial, fix for problems with respect to criterion b is provided by the choice of mixing function used to introduce or remove a given Hamiltonian. Careful work has been done on this in the context of alchemical TI involving Lennard-Jones and Coulomb forces,[32] which was broadly followed here: the essence of the strategy is to use polynomial mixing functions such that, as the ability of a given Hamiltonian $\mathcal{H}$ to direct the system into its own minima drops with $f(\lambda)$, the generalized force $\mathcal{H}\partial/(\partial\lambda)f(\lambda)$ also drops. The choice of mixing function must be balanced between criteria b and d.

Criterion c is addressed here by defining $\mathcal{H}_1$, the CS Hamiltonian, with few and low energetic barriers over the difficult ($\lambda < 0.5$) part of the integration, such that exploration is relatively quick. It has been suggested that it might also sometimes be valuable to retain barriers in the landscape as these can serve to reduce the effective dimensionality of the configurational space and actually accelerate exploration;[33] however this effect was not observed here.

Criterion d is addressed here by choosing a relatively low-order mixing function compared to some of those which have been tried in other work.[32]

Guide Hamiltonian. To manage the changes of the topology of the free energy landscape over the integration, a third Hamiltonian, $\mathcal{H}_{\text{guide}}$, was introduced in addition to $\mathcal{H}_0$ and $\mathcal{H}_1$, with a mixing function such that it would be zero at both end points of the path. The weak short-range interparticle repulsion provided by $\mathcal{H}_{\text{guide}}$ controlled the topology in the sense that it was used to first introduce gently sloping energy barriers around those states which would later take on infinite energy becoming topological "cavities" in the free energy landscape. The unshielded existence of such a cavity is intolerable if carrying out MD, because this leads to infinite values for the forces between particles.

This use of a guide Hamiltonian, introduced here, is an alternative to the practice of adding a λ dependence to the functional form of the Lennard-Jones (LJ) potential such that it is finite over all configurations for $\lambda > 0$, known as "softcoring."[34] Softcoring of the LJ typically follows mixing-out of the Coulomb interaction (which also has a discontinuity at zero separation), in a multistep procedure which increases computational expense. Such a process is also undesirable because it has the potential to introduce first order phase transitions: the phase diagram of water, for instance, is dramatically altered when electrostatics are removed. Initial attempts were made to softcore the Coulomb and LJ terms together in such a way as to preserve the shape of the energy landscape, and this was found to be prohibitively complex, especially given the requirement for the sake of efficiency to treat the Coulomb interactions using a fast algorithm such as the Ewald sum.

The use of $\mathcal{H}_{\text{guide}}$ has the advantages of solving at a stroke discontinuities of both LJ and Coulomb forces, of being extremely simple to implement and to parametrize, and of introducing no extra code into the complex and highly optimized nonbonded force and Ewald sum routines of the molecular dynamics program. The short-range repulsion is handled using a neighbor list and therefore adds only a small (and linearly scaling) cost to the calculation.

The guide Hamiltonian was defined very simply as a quadratic repulsive potential between all heavy atoms, where the cutoff R_{ij} was defined as the radius giving the minimum of the van der Waals interaction for the given atom pair ij, multiplied by 0.88.

$$\frac{\mathcal{H}_{\text{guide}}}{k_{\text{B}}T} = 20\sum_{i=1}^{N}\sum_{j=i+1}^{N}\left(\frac{\text{MIN}[R_{ij} - r_{ij}, 0]}{R_{ij}}\right)^2 \tag{4}$$

Mixing Function Design. Numerical smoothness of the integration over λ depends critically on the choice of mixing functions used to turn the Hamiltonians $\mathcal{H}_0$, $\mathcal{H}_1$, and $\mathcal{H}_{\text{guide}}$ off and on. The mixing functions were defined as polynomials:

$$f_0(\lambda) = (1 - \lambda)^4 \tag{5}$$

$$f_1(\lambda) = \lambda^2 \tag{6}$$

$$f_{\text{guide}}(\lambda) = \frac{729}{16}\lambda^2(1 - \lambda)^4 \tag{7}$$

The choice of polynomial mixing functions (which has been advised with order 4 or greater for alchemical transformations involving Lennard-Jones atoms[32]) gives generalized forces $\partial/(\partial\lambda)f_0(\lambda)\mathcal{H}_0$ and $\partial/(\partial\lambda)f_1(\lambda)\mathcal{H}_1$, which are zero for $\lambda = 1$ and $\lambda = 0$, respectively, so that (for example) two particles can pass through each other without causing a singularity in the generalized force with respect to $\mathcal{H}_0$.

Formally, the use of a polynomial mixing function is enough to stabilize the integration, mixing the two topologically distinct landscapes without an introduction of singularities. Unfortunately the multiplication of very large by very small numbers is numerically abhorrent; therefore the guide Hamiltonian was also required.

In order to allow $\mathcal{H}_{\text{guide}}$ to take effect before removing the nonsmooth Hamiltonian $\mathcal{H}_0$, the mixing function $f_0(\cdot)$ was rescaled such that the end point of the mixing would be at $\lambda = \lambda_{\text{g}}$ instead of at $\lambda = 1$ (with λ_{g} chosen arbitrarily as 0.5). The actual function used in place of $f_0(\cdot)$ was therefore $g_0(\lambda) = \text{MIN}[f_0(\lambda/(\lambda_{\text{g}})),0]$. The three mixing functions are shown in Figure 3.

METHODS

AMBER Setup. A molar NaCl concentration was defined as the ratio of Na^+ ions to H_2O molecules multiplied by the molarity of water, 55.55. $\mathcal{H}_0$ was defined using the AMBER99 force field[35] with the Barcelona corrections to nucleic acid parameters,[1] the Joung–Cheatham ion parameters,[36] and the TIP3P water model.[37] Water molecules were kept rigid using

dx.doi.org/10.1021/ct3005968 | J. Chem. Theory Comput. 2013, 9, 679–686

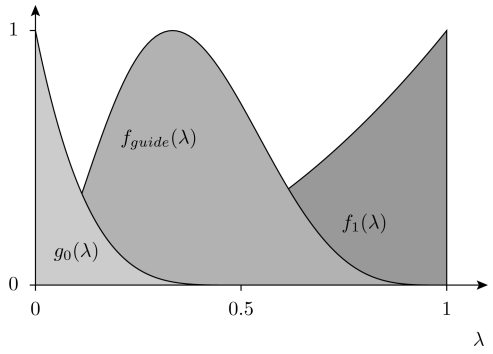

Figure 3. The three mixing functions. The function $g_0(\lambda)$ controlled the AMBER Hamiltonian $\mathcal{H}_0$. $f_1(\lambda)$ controlled the analytically tractable reference Hamiltonian $\mathcal{H}_1$, and $f_{guide}(\lambda)$ controlled the "path" Hamiltonian $\mathcal{H}_{guide}$.

the SHAKE algorithm. The temperature was held at 300 K using a Langevin thermostat with a coupling of 0.1 ps^{-1}. The seeds for the noise generator in the Langevin thermostat were set to be the same for each pair of B and Z at a given λ and [NaCl], in the hope of reaping some benefits by covariant sampling[38] in the estimate of the free energy difference. The molecular dynamics time step was 2 fs. The "pmemd" dynamics engine[39] provided in AMBER was used (with default parameters) to treat the electrostatic and other terms of the force field efficiently.

Starting configurations of $[d(CG)]_6$ DNA double helices in the B and Z conformations were prepared using the NAB molecular building tool.[40] Counterions were added near the DNA using the Xleap component of AMBER so as to neutralize backbone charge, and further counterions were then added at random to bring the salt concentration up to the required molarity assuming 9441 water molecules. Water molecules were then added from a pre-equilibrated water box, deleting those which overlapped with an ion or DNA atom, until 9441 were present. The concentrations studied were 1.11, 1.61, 2.11, and 2.61 M NaCl. The initial configurations were energy-minimized and then equilibrated at 300 K and 1 atm in the NPT ensemble for 2 ns. The average volume of each system 1.11−2.61 M NaCl was taken over the interval 1−2 ns, and the system box sizes in each configuration were set to these average volumes, so that the TI calculations could be carried out in the NVT rather than NPT ensemble.

Exploratory runs for concentrations 1.11 to 2.61 M NaCl were made out to 20 ns to check the stability and to estimate the important time and length scales of the dynamics (see the Supporting Information). Although the full TI calculations were not carried out at 2.86 M NaCl, an initial 10 ns test equilibration run was also made at this concentration (see the Supporting Information). Molecular images were prepared using VMD.[41]

Analytical Model Setup. In the reference model of the system, all solute atoms (including hydrogens) were placed in harmonic wells of spring constant $5k_BT$ $Å^{-2}$. Counterions and water oxygen atoms were assigned to three sets of identical CS wells. Because the TIP3P water molecules are treated as rigid triangles, it was not necessary to restrain the water hydrogen atoms in addition to the oxygens. The CS wells had a spring constant of $1.112k_BT$ $Å^{-2}$ up to r_1 = 1 Å, then a constant force of $1.11k_BT$ $Å^{-1}$ out to r_2 = 5 Å. The "cage-swapping" reassignment of CS wells was carried out using a Metropolis MC algorithm. For each liquid molecule present in the system, five MC well-swapping attempts were made every time step. Each system run under a mixed Hamiltonian was allowed 500 ps (250 000 time steps) of equilibration, before collecting the generalized force time series for a minimum further 500 ps, depending on convergence.

RESULTS

The equilibrium work done on each integration path is shown in Table 1.

Table 1. Equilibrium Work over Each Integration Path and Estimated Standard Errors

[NaCl]	ΔA_B (k_BT/bp)	ΔA_Z (k_BT/bp)
1.11 M	3497.21 (±0.41)	3495.60 (±0.40)
1.61 M	4123.90 (±0.41)	4123.20 (±0.40)
2.11 M	4751.90 (±0.42)	4750.93 (±0.42)
2.61 M	5378.15 (±0.43)	5378.35 (±0.44)

Free Energies. Free energies were separately calculated for Z and B conformations over a range of salt concentrations (Table 1 and Figure 4). The crossover between the B and Z

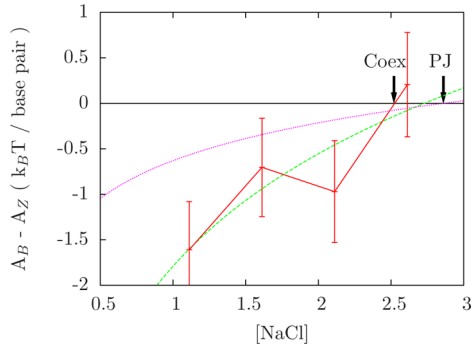

Figure 4. Free energy differences between the B and Z conformations with respect to salt concentration. The coexistence point found experimentally[10] is indicated with an arrow (PJ). The dotted line is a fit by Pohl[27] to experimental data (eq 1); the dashed line is a fit of the same function to our own data.

regimes occurred around 2.5 M NaCl, quite near the 2.86 M found in the experiments of Pohl and Jovin.[10] As far as the authors are aware, this is the most accurate numerical calculation of the coexistence position (without fitting free parameters) to date.

The shape of the free energy difference away from coexistence does not seem to match the phenomenological equation proposed by Pohl[27](eq 1); however given the small number of points and the large error bars, it is also difficult to completely discount this equation, or to suggest an alternative, more complex functional form such as from more recent theory[42,43] and experiments,[28,29] suggesting the existence of intermediates. A fit of eq 1 with A and C free gives A = 1.8 ± 0.7 and the coexistence value C = 2.7 ± 0.6 M, although, because of the questionable agreement of the shape of eq 1 with our data, we prefer to report coexistence as 2.5 M based simply on the y intercept of the trace between points three and four.

A possible explanation for the apparent overestimate of the free energy penalty for disfavored forms (the large value of the fitting parameter A) relative to the experimental data, could be

dx.doi.org/10.1021/ct3005968 | J. Chem. Theory Comput. 2013, 9, 679−686

that the experimentally studied left-handed DNA structures at low salt are not the same as the conventional Z-DNA structure observed at high salt, which was used as the starting configuration for the simulations at low salt. If the starting configurations used were in fact strongly metastable with respect to some lower-energy left-handed form (as well as with respect to the still-lower B-DNA), then this would explain the observed behavior. A wider-ranging examination of the free energy landscape would be required to discuss this possibility further.

It was found that, while the Z-DNA structure used was strongly metastable at low salt concentrations, the more labile B-DNA structure tended to melt or fray at 2.86 M NaCl and above (see Supporting Information). The greater flexibility of B-DNA, or the sharp elbow in the free energy difference above coexistence which has been suggested,[22] might serve to explain this. Given that the Watson−Crick bonded B-DNA structure was unstable with respect to a disordered structure, the TIES calculation of this paper would have been difficult to apply without artificially enforcing W−C base pairing. Separate from the difficulty of such a calculation would be the question of its interpretation in a regime where it is no longer clear that B is the dominant right-handed metastable conformation.

Integration Path. The character of the integration path can be seen by examining the generalized force due to each of the three Hamiltonians with respect to λ (Figure 5). The

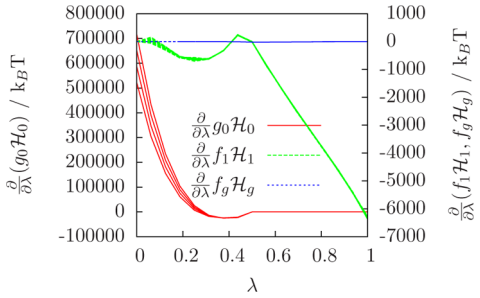

Figure 5. Generalized forces due to the AMBER Hamiltonian ($\mathcal{H}_0$), the EM+CS Hamiltonian ($\mathcal{H}_1$), and the "guide" Hamiltonian used to prevent particle overlaps during the midsection of the integration ($\mathcal{H}_g$). The guide Hamiltonian (right axis) was much smaller than the main Hamiltonians (left and right axes). A trace is shown for each of the eight calculations carried out; however B and Z cannot be distinguished on the scales used.

smoothness of these curves (apart from at $\lambda = 0.5$, where the integration-out of the AMBER Hamiltonian is completed) indicates that no first-order phase transitions were crossed during the integration path and also serves to justify the use of a basic Simpson's rule integration scheme, carried out separately over the three terms of the generalized force and over the [0, 0.5] and [0.5, 1.0] intervals.

PERFORMANCE AND CONVERGENCE

Calculations were carried out using four 2.26 GHz processor cores per integration point (therefore, 68 per measurement of $A_B - A_Z$). Calculations required on average 26.3 h per 100 ps block, giving a total of 210 000 core hours for the entire calculation (42 core months assuming 24/7 operation), plus equilibration.

To estimate the convergence of the individual generalized force measurements at each integration point, a spectral analysis of the time series of generalized forces was carried out using the CODA library of R functions,[44] in order to identify the decorrelation times and effective numbers of independent samples present. Estimated Standard Errors of the mean (ESE) are given as the root of the variance divided by the effective number of independent samples. The ESE at each value of λ (Figure 6b) provides a description of the efficiency of the sampling in each of the "mixed" free energy landscapes which were visited.

The radically different sampling efficiencies at the different integration points derive from separately addressable causes, the signatures of which are individually labeled in Figure 6, and which are discussed in relation to the criteria for good TI design which were presented above:

a. Smoothness of Generalized Force with Respect to λ. The smoothness criterion was met quite well (Figure 5).

b. Small Variance of Generalized Force. When the potential corresponding to a given term of the generalized force is very different from the potential which is controlling the dynamics, then fluctuations in that term of the force can become very large. The peak labeled "4" in Figure 6 shows this effect.

Peak "4" is lower than in first attempts, thanks to the use of a polynomial mixing function, and also greatly diminished by the use of the guide Hamiltonian. Peak "4" might also be further reduced by the use of different $\mathcal{H}_1$ Hamiltonians which more closely mirror the dynamics of the "real" $\mathcal{H}_0$ system.

c. Fast Exploration. The peaks labeled "2" and "3" show slow exploration due to roughness of the potential energy landscape: sampling of the Boltzmann distribution for atomistic models of biomolecules is famously difficult, due to the many traps and barriers which exist. Sampling also becomes slower in the CS Hamiltonian when it is fully turned on, due to the depth of the wells becoming greater than the thermal energy. Peak "5" shows a slowing of exploration due to the decoupling of particles under the CS Hamiltonian: when the particles no longer interact, decorrelation over time must rely purely on the Langevin thermostat rather than being assisted by the chaotic properties of the many-body Hamiltonians. Although the aspect indicated by peak "5" seems to be of relatively minor importance, it should be possible to address it by altering the coupling parameter of the Langevin thermostat for different values of λ, or by using an $\mathcal{H}_1$ which has explicit interparticle forces while remaining tractable.

To address point c, there is no easy escape from the need to sample the atomistic model at one end of the integration ("2"). At the other end of the integration ("3"), the trapping due to the CS potential could (and probably should) be reduced in a future calculation simply by holding the CS potential constant for $\lambda > 0.5$.

d. Near-Linear Mixing. Peak "1" arises because the gradient of the mixing function $g(\lambda)$ is large at small λ, and this large value scales not only the generalized force but its variance—this represents a trade-off accepted in the process of mixing function selection; it stands in balance against peak "4."

To address this need to trade between the criteria b and d, it seems that the best hope is to improve the guide or end point Hamiltonians used such that the need for a polynomial mixing function is removed.

dx.doi.org/10.1021/ct3005968 | J. Chem. Theory Comput. 2013, 9, 679−686

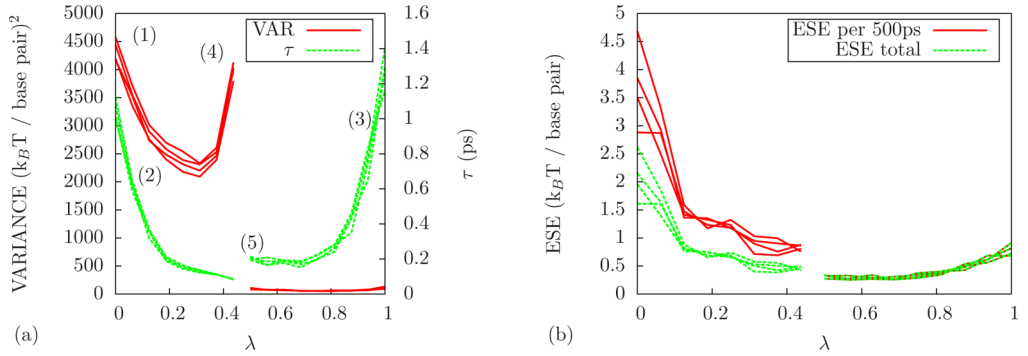

Figure 6. (a) Variance and decorrelation time of generalized force. The rate of convergence of the estimate of the summed generalized force (B−Z) at a given λ was determined by variance (left axis, red) and by the decorrelation time τ (right axis, green). Numbered labels indicate peaks in the variance or in τ, which are discussed individually in the text. (b) ESE of the generalized force. The ESE per 500 ps was much higher for $\lambda < 0.5$; therefore longer runs of 1600 ps were made for this section. A separate trace is shown for each salt concentration studied. Lines are not drawn between the points at $\lambda = 7/16$ and $\lambda = 8/16$ because the generalized forces on the two intervals $\lambda < 0.5$ and $\lambda \geq 0.5$ had different shapes and were integrated separately. Each trace corresponds to the ΔA calculation for a given [NaCl].

DISCUSSION

This calculation is the most quantitatively accurate numerical estimate of the salt concentration at B−Z DNA coexistence to date. As recently as 2010, it was noted that an atomistic calculation of this value should be prohibitively difficult "because the problem requires the sampling of an extraordinarily large configuration space, including water and ions, to obtain the free energy difference";[18] that the result is quantitatively correct demonstrates solid improvements in the techniques of free energy estimation suitable for biomolecular complexes, over and above the normal progress due to improved hardware.

Because of the reductive nature of the molecular dynamics approach (treating, for instance, an atom in a protein in much the same way as an atom in a DNA base), it is reasonable to assume that the software and parameter sets developed can be reused widely and can be effective for any combination of protein, nucleic acid, counterions, and solvent, although there is still substantial room for further development of them. It is intended to release the software and parameter sets as a downloadable library on Dr. Berryman's Web site, for easy linking against the AMBER simulation program or other packages.

The accuracy of the final result for the coexistence serves as a validation for use of the combination of the Joung−Cheatham ion parameters and the parmbsc force field (both of which are relatively new) with TIP3P water for the simulation of DNA under the fairly unusual conditions of very high salt concentration.

The work here has made minor alterations to the "cage-swapping" model for absolute free energy calculation of fluids and combined it with a standard Einstein molecule method for the solute. The principal novelty was in the scale and complexity of the system treated, but the introduction of a "guide" Hamiltonian to control the path of the thermodynamic integration while not altering behavior at the end points is also novel as far as the authors are aware.

There is too much active research in thermodynamic integration and free-energy perturbation methods to give a comprehensive list of ideas which could influence further work. A brief suggestion is that absolute free energy methods could be well suited to the mapping of phase diagrams of complex fluids. There are a large number of biomolecular and soft-matter systems which exhibit rich phase behavior that have not yet been explored. On the methodological side, recent advances in nonequilibrium TI,[45] in correlated sampling and in Hamiltonian exchange[46] all offer increases in computational efficiency for future TIES calculations. It has been suggested that an efficiency gain can be made by doing away with the intermediate stages of the TI calculation entirely, instead carrying out a type of importance sampling over $\mathcal{H}_0$ and $\mathcal{H}_1$ such that those areas of configurational space which overlap between them receive enhanced attention.[47]

If one is interested in locating a phase transition, one can, of course, use eq 3 to compute the free energy difference between two phases directly and avoid the "detour" via absolute free energies; however, eq 3 only holds if the integration path does not cross a first order phase transition. TIES is thus more generally useful (compared to performing TI over single or multilegged free energy cycles between nontractable Hamiltonians) in that states which are separated by a first order phase transition can be compared. This is much simpler than carrying out TI calculations which integrate between phases by following a complex path designed to give consistently pseudocritical behavior.[2,48]

A second general argument for TIES, which is more germane for the specific calulation presented here, is that setting one end point of the integration as an analytically tractable model leaves open the possibility of a shorter and smoother integration path, with smaller variances in the generalized force at a given λ, as the analytical models are refined. The most obvious step in further development, then, is extension and refinement of the analytical models which serve as end points for the calculation. Ideally, the mixed energy landscapes generated by an analytically tractable model should be as similar as possible to "softened" versions of the initial Hamiltonian. This possibility should serve as a call to arms for any theorists who may believe that they can swiftly assemble a tractable model for some system of interest.

ASSOCIATED CONTENT

Supporting Information

A supporting document is provided, giving derivations for the absolute free energies of the CS and EM Hamiltonians. A second supporting document showing convergence of the simulations is also provided. This material is available free of charge via the Internet at http://pubs.acs.org.

dx.doi.org/10.1021/ct3005968 | J. Chem. Theory Comput. 2013, 9, 679−686

AUTHOR INFORMATION

Corresponding Author

*E-mail: josh.berryman@uni.lu.

Notes

The authors declare no competing financial interest.

ACKNOWLEDGMENTS

This work was greatly assisted by discussions with Charles Laughton and Sarah Anne Harris. Computing was provided by the HPC facility of the University of Luxembourg and by the European Soft Matter Infrastructure program.

REFERENCES

(1) Pérez, A.; Marchán, I.; Svozil, D.; Sponer, J.; Cheatham, T. E.; Laughton, C. A.; Orozco, M. *Biophys. J.* **2007**, *92*, 3817−3829.
(2) Eike, D. M.; Maginn, E. J. *J. Chem. Phys.* **2006**, *124*, 164503.
(3) Tyka, M. D.; Sessions, R. B.; Clarke, A. R. *J. Phys. Chem. B* **2007**, *111*, 9571−9580.
(4) Cecchini, M.; Krivov, S. V.; Spichty, M.; Karplus, M. *J. Phys. Chem. B* **2009**, *113*, 9728−9740.
(5) Schilling, T.; Schmid, F. *J. Chem. Phys.* **2009**, *131*, 231102.
(6) Frenkel, D.; Ladd, A. J. C. *J. Chem. Phys.* **1984**, *81*, 3188−3193.
(7) Vega, C.; Noya, E. G. *J. Chem. Phys.* **2007**, *127*, 154113.
(8) Schmid, F.; Schilling, T. *Phys. Procedia* **2010**, *4*, 131−143.
(9) Case, D. A.; Darden, T. A.; Cheatham, T. E.; Simmerling, C. L.; Wang, J.; Duke, R. E.; Luo, R.; Crowley, M.; Walker, R. C.; Zhang, W.; Merz, K. M.; Wang, B.; Hayik, S.; Roitberg, A.; Seabra, G.; Kolossváry, I.; Wong, K. F.; Paesani, F.; Vanicek, J.; Wu, X.; Brozell, S. R.; Steinbrecher, T.; Gohlke, H.; Yang, L.; Tan, C.; Mongan, J.; Hornak, V.; Cui, G.; Mathews, D. H.; Seetin, M. G.; Sagui, C.; Babin, V.; Kollman, P. A. *Amber 11*; University of California: San Francisco, 2010.
(10) Pohl, F. M.; Jovin, T. M. *J. Mol. Biol.* **1972**, *67*, 375−396.
(11) Ferreira, J. M.; Sheardy, R. D. *Biophys. J.* **2006**, *91*, 3383−3389.
(12) Oh, D.-B.; Kim, Y.-G.; Rich, A. *Proc. Natl. Acad. Sci. U. S. A.* **2002**, *99*, 16666−16671.
(13) Peck, L. J.; Nordheim, A.; Rich, A.; Wang, J. C. *Proc. Natl. Acad. Sci. U. S. A.* **1982**, *79*, 4560−4564.
(14) Wang, G.; Christensen, L. A.; Vasquez, K. M. *Proc. Natl. Acad. Sci. U. S. A.* **2006**, *103*, 2677−2682.
(15) Kastenholz, M. A.; Schwartz, T. U.; Hünenberger, P. H. *Biophys. J.* **2006**, *91*, 2976−2990.
(16) Lee, J.; Kim, Y.-G.; Kim, K. K.; Seok, C. *J. Phys. Chem. B* **2010**, *114*, 9872−9881.
(17) Behe, M.; Felsenfeld, G. *Proc. Natl. Acad. Sci. U. S. A.* **1981**, *78*, 1619−1623.
(18) Maruyama, Y.; Yoshida, N.; Hirata, F. *J. Phys. Chem. B* **2010**, *114*, 6464−6471.
(19) Kollman, P.; Weiner, P.; Quigley, G.; Wang, A. *Biopolymers* **1982**, *21*, 1945−1969.
(20) Misra, V. K.; Honig, B. *Biochemistry* **1996**, *35*, 1115−1124.
(21) Guéron, M.; Demaret, J.; Filoche, M. *Biophys. J.* **2000**, *78*, 1070−1083.
(22) Soumpasis, D. M. *Proc. Natl. Acad. Sci. U. S. A.* **1984**, *81*, 5116−5120.
(23) Jovin, T. M.; Soumpasis, D. M.; McIntosh, L. P. *Annu. Rev. Phys. Chem.* **1987**, *38*, 521−558.
(24) Montoro, J. C. G.; Abascal, J. L. F. *J. Chem. Phys.* **1997**, *106*, 8239−8253.
(25) Hirata, F.; Levy, R. M. *J. Phys. Chem.* **1989**, *93*, 479−484.
(26) Shannon, R. D. *Acta Crystallogr., Sect. A* **1976**, *32*, 751−767.
(27) Pohl, F. M. *Cold Spring Harbor Symp. Quant. Biol.* **1983**, *47*, 113−117.
(28) Ivanov, V. I.; Karapetian, A. T.; Miniat, E. E.; Sad', I. *Mol. Biol. (Mosk.)* **1993**, *27*, 1150−1156.
(29) Grzeskowiak, K.; Ohishi, H.; Ivanov, V. *Nucleic Acids Symp. Ser.* **2005**, 249−250.
(30) Reinhard, F.; Grubmüller, H. *J. Chem. Phys.* **2007**, *126*, 014102.
(31) LaBerge, L. J.; Tully, J. C. *Chem. Phys.* **2000**, *260*, 183−191.
(32) Steinbrecher, T.; Mobley, D. L.; Case, D. A. *J. Chem. Phys.* **2007**, *127*, 214108.
(33) McLeish, T. *Biophys. J.* **2005**, *88*, 172−183.
(34) Beutler, T. C.; Mark, A. E.; van Schaik, R. C.; Gerber, P. R.; van Gunsteren, W. F. *Chem. Phys. Lett.* **1994**, *222*, 529−539.
(35) Wang, J.; Cieplak, P.; Kollman, P. A. *J. Comput. Chem.* **2000**, *21*, 1049−1074.
(36) Joung, I. S.; Cheatham, T. E. *J. Phys. Chem. B* **2008**, *112*, 9020−9041.
(37) Jorgensen, W. L.; Chandrasekhar, J.; Madura, J. D.; Impey, R. W.; Klein, M. L. *J. Chem. Phys.* **1983**, *79*, 926−935.
(38) Assaraf, R.; Caffarel, M.; Kollias, A. C. *Phys. Rev. Lett.* **2011**, *106*, 150601.
(39) Duke, R. E.; Pedersen, L. G. *PMEMD 3*; University of North Carolina-Chapel Hill: Chapel Hill, NC, 2003.
(40) Macke, T. J.; Case, D. A. In *Modeling Unusual Nucleic Acid Structures*; American Chemical Society: Washington, DC, 1997; Chapter 25, pp 379−393.
(41) Humphrey, W.; Dalke, A.; Schulten, K. *J. Mol. Graphics* **1996**, *14*, 33−38.
(42) Frank-Kamenetskii, M. D.; Lukashin, A. V.; Anshelevich, V. V. *J. Biomol. Struct. Dyn.* **1985**, *3*, 35−42.
(43) Lukashin, A. V.; Beglov, D. B.; Frank-Kamenetskii, M. D. *J. Biomol. Struct. Dyn.* **1991**, *8*, 1113−1118.
(44) Plummer, M.; Best, N.; Cowles, K.; Vines, K. *R News* **2006**, *6*, 7−11.
(45) Vaikuntanathan, S.; Jarzynski, C. *J. Chem. Phys.* **2011**, *134*, 054107.
(46) Khavrutskii, I. V.; Wallqvist, A. *J. Chem. Theory Comput.* **2010**, *6*, 3427−3441.
(47) Wilms, D.; Wilding, N. B.; Binder, K. *Phys. Rev. E* **2012**, *85*, 056703.
(48) Grochola, G. *J. Chem. Phys.* **2004**, *120*, 2122−2126.